Molecular Pharmacology Fast Forward. Published on May 20, 2013 as DOI: 10.1124/mol.113.085852
This article has not been copyedited and formatted. The final version may differ from this version.

Mol #85852

Molecular Insights into Microbial β-Glucuronidase Inhibition to Abrogate CPT-11 Toxicity

Adam B. Roberts, Bret D. Wallace, Madhu Kumar Venkatesh, Sridhar Mani,

and Matthew R. Redinbo

Departments of Biochemistry, Chemistry and Microbiology, University of North Carolina at Chapel Hill (ABR, BDW, MRR)

Department of Medicine, Einstein College of Medicine (MKV, SM)

Molecular Pharmacology Fast Forward. Published on May 20, 2013 as DOI: 10.1124/mol.113.085852
This article has not been copyedited and formatted. The final version may differ from this version.

Running Title: Bacterial β-glucuronidase inhibitors alleviate drug toxicity

Address Correspondence to:

Matthew R. Redinbo
Campus Box #3290
University of North Carolina at Chapel Hill
Chapel Hill, NC 27599-3290
redinbo@unc.edu

Text pages: 27

Number of tables: 2

Number of figures: 7

Number of references: 51

Number of words in Abstract: 222

Number of words in Introduction: 732

Number of words in Discussion: 830

Abbreviations: BSA, body surface area; CE, carboxylesterase; CPT-11, 7-ethyl-10-[4-(1-piperidino)-1-piperidino]; DMEM, Dulbecco's modified Eagle's medium; DMSO, dimethyl sulfoxide GI, gastrointestinal; HB101, chemically competent *E. coli* cells; HCT116, human colon carcinoma cells; PEG-3350, polyethylene glycol 3350; PNP, p-nitrophenol; PNPG, p-nitrophenyl β-D-glucuronide; SN-38, 7-ethyl-10-hydroxycamptothecin; SN-38G, SN-38 glucuronide; UGT, UDP-glucuronosyltransferase.

Molecular Pharmacology Fast Forward. Published on May 20, 2013 as DOI: 10.1124/mol.113.085852
This article has not been copyedited and formatted. The final version may differ from this version.

Abstract

Bacterial β-glucuronidases expressed by the symbiotic intestinal microbiota appear to play important roles in drug-induced epithelial cell toxicity in the gastrointestinal (GI) tract. For the anticancer drug CPT-11 (Irinotecan) and the non-steroidal anti-inflammatory drug diclofenac, it has been shown that removal of the glucuronide moieties from drug metabolites by bacterial β-glucuronidases in the GI lumen can significantly damage the intestinal epithelium. Furthermore, selective disruption of bacterial β-glucuronidases by small molecule inhibitors alleviates these side effects, which, for CPT-11, can be dose-limiting. Here we characterize novel microbial β-glucuronidase inhibitors that inhibit *E. coli* β-glucuronidase *in vitro* with K_i values between 180 nM and 2 μM, and disrupt the enzyme in *E. coli* cells with EC_{50} values as low as 300 nM. All compounds are selective for *E. coli* β-glucuronidase without inhibiting purified mammalian β-glucuronidase, and they do not impact the survival of either bacterial or mammalian cells. The 2.8 Å resolution crystal structure of one inhibitor bound to *E. coli* β-glucuronidase demonstrates that it contacts and orders only a portion of the "bacterial loop" present in microbial, but not mammalian, β-glucuronidases. The most potent compound examined in this group was found to protect mice against CPT-11-induced diarrhea. Taken together, these data advance our understanding of the chemical and structural basis of selective microbial β-glucuronidase inhibition, which may improve human drug efficacy and toxicity.

Molecular Pharmacology Fast Forward. Published on May 20, 2013 as DOI: 10.1124/mol.113.085852
This article has not been copyedited and formatted. The final version may differ from this version.

Introduction

CPT-11 (Irinotecan, 7-ethyl-10-[4-(1-piperidino)-1-piperidino]) is employed worldwide for the treatment of a variety of solid malignancies, but its efficacy is often limited by severe GI toxicity (Rothenberg et al., 1996; Rougier et al., 1997; Cunningham et al., 1998; Rougier et al., 1998; Saltz et al., 2000; Fuchs et al., 2003; Hu et al., 2006; Kurita et al., 2011). CPT-11 is most frequently utilized in first- and second-line treatment of metastatic colon cancers, typically in combination with other agents (Smith et al., 2006; Kambe et al., 2012). More recently, CPT-11 has been employed in preclinical and clinical trials against a range of other neoplasticities, including brain tumors, lung, breast, gastric, pancreatic, and gynecological cancers (Matsumura et al., 2010; Han et al., 2012; Jo et al., 2012; Kim et al., 2012; Spigel et al., 2012; Zaniboni et al., 2012; Lee et al., 2013).

CPT-11 is a prodrug that is converted to SN-38 (7-Ethyl-10-hydroxy-camptothecin) by carboxylesterase (CE) enzymes. SN-38, the active metabolite of CPT-11, induces anti-tumor effects by poisoning the human topoisomerase I catalytic cycle, leading to cell death (Kawato et al., 1991; Mathijssen et al., 2001; Ma and McLeod, 2003). The fate of SN-38 *in vivo* is further regulated by UDP-glucuronosyltransferase (UGT) enzymes in the liver and other tissues. UGT isoforms, in particular UGT1A1, catalyze the conjugation of a glucuronide group onto SN-38, producing the inactive compound SN-38 glucuronide (SN-38G), which is marked for elimination through the bile and into the GI tract (Nagar and Blanchard, 2006). However, as SN-38G passes through the GI tract, it acts as a substrate for bacterial β-glucuronidases present in intestinal symbiotic microbes (Tobin et al., 2003; Stein et al., 2010). These enzymes, in turn, reactivate SN-38 *in situ,* resulting in toxic injury to the intestinal epithelial cells (Araki et al., 1993). Indeed, the severity of CPT-11-induced diarrhea is correlated with levels of β-

Molecular Pharmacology Fast Forward. Published on May 20, 2013 as DOI: 10.1124/mol.113.085852
This article has not been copyedited and formatted. The final version may differ from this version.

glucuronidase activity in the intestinal lumen, and the intestinal microbiota have been found to play an important role in the development of this toxicity (Takasuna et al., 1996; Takasuna et al., 1998; Mathijssen et al., 2001; Brandi et al., 2006). While most early-onset diarrhea associated with CPT-11 treatment can be treated with anti-motility agents, the delayed GI toxicity associated with SN-38 can be refractory to standard treatments (Saliba et al., 1998). It has now been convincingly demonstrated that the intestinal toxicity of CPT-11 limits dose intensification and optimized delivery of CPT-11 (Abigerges et al., 1994; Ducreux et al., 2003; Zhao et al., 2004).

The role microbial enzymes expressed by symbiotic bacteria play in therapeutic metabolism has been appreciated since the early days of drug discovery (Sousa et al., 2008). We recently hypothesized that selective microbial β-glucuronidase inhibitors would alleviate CPT-11-induced toxicity. *In vitro* and cell-based assays demonstrated that a set of chemically similar compounds identified by high-throughput screening displayed potent inhibition of *E. coli* β-glucuronidase and did not impact the viability of cultured bacterial or mammalian cells (Wallace et al., 2010). Crystal structures of inhibitors in complex with *E. coli* β-glucuronidase reveal that the small molecules bind to a loop present in bacterial β-glucuronidases but missing in the mammalian orthologs; accordingly, the inhibitors examined had no inhibitory effect *in vitro* on a mammalian β-glucuronidase (Wallace et al., 2010). Oral administration of one of the inhibitors to mice alleviated CPT-11-induced diarrhea and intestinal damage (Wallace et al., 2010). Furthermore, in a subsequent study, the administration of the same inhibitor protected mice from small intestinal ulceration caused by the non-steroidal anti-inflammatory drug diclofenac, which is also subject to glucuronidation and reactivation in the intestinal lumen (LoGuidice et al., 2012).

Here we describe the inhibitory profile of four novel inhibitors that are chemically distinct from the originally reported set (Wallace et al., 2010; Ahmad et al., 2011). These compounds are shown to be *in vitro* inhibitors of *E. coli* β-glucuronidase but are non-lethal to cultured *E. coli*

Molecular Pharmacology Fast Forward. Published on May 20, 2013 as DOI: 10.1124/mol.113.085852
This article has not been copyedited and formatted. The final version may differ from this version.

and mammalian cells. The x-ray crystal structure of *E. coli* β-glucuronidase in complex with one of the inhibitors reveals that it binds to the entrance of the enzyme's active site and makes contact with, but does not completely order, the flexible "bacterial loop" unique to the microbial β-glucuronidases. We also show that the most potent of these new compounds protects mice from CPT-11-induced diarrhea. Taken together, these data enhance our understanding of the selective modulation of microbial β-glucuronidases, which may lead to the targeted alleviation of drug-induced toxicity in the human GI tract.

Materials and Methods

Expression and Purification of E. coli β-Glucuronidase. *E coli* β-glucuronidase (EC 3.2.1.31) was expressed and purified as described previously (Wallace et al., 2010). Purified *E coli* β-glucuronidase was stored in 20 mM HEPES, 50 mM NaCl, pH 7.4 at ~10 mg/mL at -80^{o}C. The Δ360-376 form of *E. coli* β-glucuronidase was created using PCR mutagenesis, confirmed by sequencing, and purified as described previously (Wallace et al., 2010).

Inhibitor Compounds. Compounds (Figure 1) identified from high-throughput screening (Wallace et al., 2010; Ahmad et al., 2011) were purchased from ASINEX, Inc, Moscow, Russia. Each compound was provided as a solid powder and dissolved initially in 100% DMSO at 25 mM.

Kinetic and Equilibrium Inhibition Assays*.* Inhibition assays were conducted by measuring the β-glucuronidase-catalyzed conversion of p-nitrophenyl β-D-glucuronide (PNPG) to p-nitrophenol (PNP). PNPG was acquired from Sigma-Aldrich, St. Louis, MO, and stored by dissolving in water at 250 mM. The conversion of increasing concentrations of PNPG to PNP, in

Molecular Pharmacology Fast Forward. Published on May 20, 2013 as DOI: 10.1124/mol.113.085852
This article has not been copyedited and formatted. The final version may differ from this version.

the presence of 10 nM enzyme, was measured in the presence of increasing concentrations of our putative inhibitors; zero-substrate and zero-inhibitor controls were carried out at the same time. Reactions were conducted in 96-well, clear-bottom assay plates (Costar, Tewksbury, MA) at 37^{o}C in 50 µL of total volume. The reaction consisted of 10 µL of assay buffer (5% DMSO and 500 mM HEPES, pH 7.4), 5 µL of inhibitor solution (various concentrations), 5 µL of 100 nM enzyme, and 30 µL of substrate (various concentrations). Product formation was calculated by measuring the change in absorbance over time at 410 nm using a PHERAstar *Plus* microplate reader (BMG Labtech, Ortenberg, Germany). The acquired data were analyzed using Microsoft Excel and Sigmaplot 11.0. From these data, K_i values were calculated for each of the inhibitors.

A related assay was employed to calculate the IC_{50} values in the following manner. An analogous 50 µL reaction, consisting of enzyme (1 nM final), buffer, PNPG (1 mM final), and variable concentrations of the inhibitors, was incubated at 37^{o}C for 6 hours to allow the reaction to reach equilibrium and then quenched with 100 µL 0.2 M sodium carbonate. The percent inhibition for each concentration of inhibitor was calculated based on changes in absorbance and used to plot a dose-response curve. The IC_{50} value was calculated as the concentration of inhibitor that produced 50% *in vitro* inhibition. The same assay was performed with purified bovine liver β-glucuronidase with PNPG as the substrate.

We also tested the ability of these compounds to inhibit β-glucuronidase in *E. coli* cells. We grew HB101 *E. coli* cells, transformed with the pET-28a vector containing the β-glucuronidase gene, to an OD_{600} of 0.6 in LB medium and used a small aliquot in an assay similar to the *in vitro* IC_{50} assay described above. The cells (39 µL) were incubated with 1 µL of variable concentrations of inhibitor and 10 µL of 1 mM PNPG at 37^{o}C for 6 hours. The reaction was quenched with 100 µL 0.2 M sodium carbonate. The amount of substrate turnover and therefore the amount of inhibition is calculated from the change in absorbance compared to zero-inhibitor controls. EC_{50} values were calculated as the amount of inhibitor necessary to produce 50%

Molecular Pharmacology Fast Forward. Published on May 20, 2013 as DOI: 10.1124/mol.113.085852
This article has not been copyedited and formatted. The final version may differ from this version.

inhibition. The *in vitro* and cell-based assays employed here were similar to those reported previously (Wallace et al., 2010).

Additional Glycosidase Enzymes. Mammalian (bovine liver) β-glucuronidase (lyophilized powder, EC 3.2.1.31), *Prunis dulcis* β-glucosidase (lyophilized powder, EC 3.2.1.21), *Helix pomatia* β-mannosidase (ammonium sulfate suspension, EC 3.2.1.25), *E. coli* β-galactosidase (lyophilized powder, EC 3.2.1.23), and bovine liver β-galactosidase (lyophilized powder, EC 3.2.1.23) were purchased from Sigma-Aldrich, St. Louis, MO. The assays were conducted as previously published, using the appropriate p-nitrophenyl-glycosidase compound as the primary substrate for enzyme activity detection (Graef et al., 1977). Each of the four inhibitors was tested for an effect on each glycosidase enzyme activity by adding a concentration range of 0 to 100 μM to the reaction mixture. The reaction was allowed to proceed for 6 hours at 37^{o}C and then quenched with 100 μL 0.2 M sodium carbonate. Absorbance was measured at the appropriate wavelength, and the data were analyzed using Microsoft Excel and SigmaPlot 11.0.

Toxicity of Inhibitors toward Cultured Cells. The toxicity of inhibitors to bacterial cells was examined by incubating HB101 *E. coli* cells, transformed with the pET-28a vector containing the β-glucuronidase gene, grown to an OD_{600} of 0.6 in LB medium with each compound, as well as DMSO and ampicillin as controls, for 6 hours. Cell survivability was measured by plating a 10^{-5} dilution of the cells on LB media enriched with kanamycin. After overnight incubation, colonies were counted to quantify cell viability. We used a similar assay to assess the inhibitor's toxicity toward cultured HCT116 human colon cancer cells, which were grown and cultured in DMEM media. Aliquots of HCT116 cells were incubated with 100 μM of each lead for 24 hours. The resulting viability of the cells was quantified by using the CellQuanti-Blue™ Cell Viability Assay Kit (BioAssay Systems, Hayward, CA). Cells are incubated with CellQuanti-Blue™ Reagent and fluorescence was measured.

Molecular Pharmacology Fast Forward. Published on May 20, 2013 as DOI: 10.1124/mol.113.085852
This article has not been copyedited and formatted. The final version may differ from this version.

Crystal Structure Determination. Crystals of *E. coli* β-glucuronidase were obtained at 2 mg/mL protein with 30-fold molar excess Inhibitor 8 (Figure 1) in 17% PEG-3350 (w/v), 250 mM magnesium acetate, and 0.02% sodium azide (w/v) at 16°C. Crystals first appeared after 5 days, and were immediately cryo-protected with perfluoropolyether vacuum pump oil (Sigma-Aldrich, St. Louis, MO) and flash-cooled in liquid nitrogen. Diffraction data were collected on the 22-BM beam line at SER-CAT (Advanced Photon Source, Argonne National Laboratory). Data in space group C2 were indexed and scaled using HKL2000 (Z. Otwinowski et al., 1997) to 2.83 Å resolution. The asymmetric unit contained two monomers. The structure was determined with Phaser (McCoy et al., 2007) using molecular replacement with the recent apo *E. coli* β-glucuronidase structure (PDB ID 3K46) as a search model. The structure was refined using simulated annealing and torsion angle refinement with the maximum likelihood function target in CNS, and monitored using both the crystallographic R and cross-validating R-free statistics (Brünger, 1997). The software suite PHENIX (Adams et al., 2002) was also employed for grouped B-factor (with two groups – main chain, and side chain) and TLS refinement. The model was manually adjusted using Coot (Emsley and Cowtan, 2004) and $2F_o$-F_c and F_o-F_c electron density maps. The ligand model and definition files were generated using PRODRG (Schüttelkopf and van Aalten, 2004), and were placed into electron density in the active site of both monomers in the asymmetric unit.

Animal Studies. Animal experiments were performed according to the Institutional Animal Care and Use guidelines approved by the Institutional Animal Care and Use Committee (IACUC # 20070715 and 20100711) of the Albert Einstein College of Medicine, Bronx, New York. CPT-11 was purchased from LC Laboratories, Woburn, MA (catalog number: I-4122) as a hydrochloride salt (> 99% HPLC purified grade). CPT-11 (20 mg/mL) and Inhibitor 5 (100 μg/mL) were dissolved in 0.25% (w/v) carboxymethylcellulose sodium salt (Sigma, C5013) to make stock

Molecular Pharmacology Fast Forward. Published on May 20, 2013 as DOI: 10.1124/mol.113.085852
This article has not been copyedited and formatted. The final version may differ from this version.

solutions. As a vehicle control, all animals received an equivalent volume (compared to experimental groups) of 0.25% (w/v) carboxymethylcellulose sodium salt solution. BALB/cJ mice female (8-10 week old) were obtained from Jackson Laboratories, Bar Harbor, ME. The mice were housed in conventional metabolic cages (N=1/cage) and kept in a room under controlled temperature (20-22^{o}C) and 12 hour day-night cycle. Animals had free access to water and conventional food without fortification. Mice were divided into four groups of 9 animals each: Group 1, vehicle controls received equivalent volume of 0.25% (w/v) carboxymethylcellulose sodium salt solution intraperitoneally (i.p.) and by oral gavage (~100 µL twice per day); Group 2, Inhibitor 5 gavaged (10 µg/day) twice per day (every 10 hours) starting on day –1 with oral gavage of 0.25% (w/v) carboxymethylcellulose sodium salt solution, and i.p. once per day; Group 3, CPT-11 injected (50 mg/kg) i.p. once daily in the morning with oral gavage of 0.25% (w/v) carboxymethylcellulose sodium salt solution; Group 4, CPT-11 injected (50mg/kg) i.p. once daily in the morning, and Inhibitor 5 gavaged (10 µg/day) twice per day (every 10 hours). Total injected volume was identical for each animal. Mice were weighed and examined daily for signs of diarrhea (fecal staining of skin, lose watery stool) and bloody diarrhea (black sticky stool). Body weight, stool consistency and blood in stool were monitored daily using methods previously published (Cooper et al., 1993; Wallace et al., 2010). Previous studies indicate that dosing at ~60-80 mg/kg/day of CPT-11 for 4 days allows for observation of delayed diarrhea around 15 days (Reagan-Shaw et al., 2008). A dosing scheme of 50 mg/kg/day, once daily for 9 days, was chosen with the intention of accelerating the onset of diarrhea while preventing death. As outlined previously, 50 mg/kg CPT-11 in mice is roughly equivalent to the 5 mg/kg typical human CPT- 11 dose based on differences in body surface area (BSA) (Brandi et al., 2006; Reagan-Shaw et al., 2008). GI symptoms in Group 3 started as early as day 2 and up to day 10, and included decreased appetite, bowel movements, mobility and body weight. All animals were euthanized on day 11.

Molecular Pharmacology Fast Forward. Published on May 20, 2013 as DOI: 10.1124/mol.113.085852
This article has not been copyedited and formatted. The final version may differ from this version.

Results

In Vitro *and Cell-Based* E. coli *β-Glucuronidase Inhibition*

Four compounds were chosen from high-throughput screening results (Wallace et al., 2010; Ahmad et al., 2011) for further functional and structural characterization (Figure 1). These compounds (Inhibitors 5-8) are relatively distinct in structure from one another, and are also distinct from the four chemically-similar compounds (Inhibitors 1-4) reported previously (Wallace et al., 2010). In *in vitro* assays with purified *E. coli* β-glucuronidase, we found that all four compounds functioned as inhibitors, with IC_{50} and K_i values ranging from 180 nM (Inhibitor 5) to 4 μM (Inhibitor 7) (Table 1), similar to those observed previously with Inhibitors 1-4 (Wallace et al., 2010). Only Inhibitors 5, 6 and 8, however, were effective against the β-glucuronidase target in living *E. coli* cells. Inhibitor 7, the weakest *in vitro* compound, showed no impact in cells, while Inhibitors 5, 8, and 6 exhibited 300 nM, 1.2 μM and 7.3 μM EC_{50} values, respectively (Table 1). The relatively potent in-cell EC_{50} values compared to the *in vitro* IC_{50} values are likely due to differences in compound entry, metabolism, export, or partitioning within living cells; such features will be examined in future studies. In summary, we have identified novel compounds that exhibit *in vitro* and in-cell inhibition of *E. coli* β-glucuronidase and this information expands our understanding of chemical moieties capable of disrupting bacterial β-glucuronidase activity.

Selectivity for Bacterial β-Glucuronidase

We next tested the ability of Inhibitors 5-8 to disrupt the activity of β-glucuronidase from bovine liver, a mammalian enzyme ortholog that processes larger glucosaminoglycan substrates relative to the bacterial β-glucuronidases (Ray et al., 1999). We found that Inhibitors

Molecular Pharmacology Fast Forward. Published on May 20, 2013 as DOI: 10.1124/mol.113.085852
This article has not been copyedited and formatted. The final version may differ from this version.

5-8 failed to impact the activity of the bovine liver enzyme at concentrations up to 100 μM (Figure 2), demonstrating that Inhibitors 5-8 are selective for the *E. coli* β-glucuronidase. We also examined the *in vitro* effects of these inhibitors on other glycosidase enzymes. We tested each inhibitor against four commercially-available enzymes: a plant β-glucosidase (from the almond tree *Prunis dulcis*), a mollusk β-mannosidase (from *Helix pomatia*), and the β-galactosidases from both *E. coli* and bovine sources. In all cases, Inhibitors 5-8 failed to exhibit inhibition at compound concentrations up to 100 μM (data not shown). Similarly, the previously reported Inhibitors 1-4 also failed to exert an effect on these glycosidases (data not shown). Thus, we conclude that the β-glucuronidases Inhibitors 1-8 are selective for the bacterial β-glucuronidase and do not inhibit either mammalian β-glucuronidase or members of the related family of sugar-cleaving enzymes from a range of sources.

Lethality to Bacterial or Mammalian Cells

Eliminating toxic drug metabolites in the GI tract by disrupting microbial β-glucuronidases requires that inhibitors are not harmful to human or bacterial cells. Indeed, it is increasingly well established that symbiotic microbiota are essential for GI health (Consortium, 2012). We tested whether Inhibitors 5-8 were lethal to cultured *E. coli* cells or HCT116 human colon cancer cells at compound concentrations up to 100 μM. We found that all four inhibitors did not affect the survival of either *E. coli* or HCT116 cells (Figure 3). Thus, they appear to satisfy the criteria that successful compounds are relatively non-toxic to bacterial cells or human epithelial cells.

Structure of **E. coli** *β-Glucuronidase Complexed with Inhibitor 8*

To further our understanding of the molecular basis of *E. coli* β-glucuronidase inhibition, we determined the 2.83 Å resolution crystal structure of the enzyme in complex with Inhibitor 8

Molecular Pharmacology Fast Forward. Published on May 20, 2013 as DOI: 10.1124/mol.113.085852
This article has not been copyedited and formatted. The final version may differ from this version.

(PDB ID 4JHZ) (Table 2). The asymmetric unit contained two β-glucuronidase monomers (Figure 4A), while C2 crystallographic symmetry produced the physiologically relevant β-glucuronidase tetramer (Wallace et al., 2010). The apo (unliganded) structure of *E. coli* β-glucuronidase was used as a molecular replacement search model to eliminate any previous ligand model bias. After careful refinement of the protein model structure, electron density at 1.0 σ level in the composite omit map was present for Inhibitor 8 in both monomers of the asymmetric unit (Figure 4B). After refinement of the atomic positions as well as their thermal displacement parameters (B-factors), the ligands had an occupancy of 0.93 and 0.91 with an average B-factors of 66.4 $Å^2$ and 76.5 $Å^2$ for chain A and B, respectively.

Inhibitor 8 was placed in an orientation that both satisfies the electron density and makes chemically reasonable interactions with the neighboring amino acid side chains. The compound binds to the entrance to the active site cleft of *E. coli* β-glucuronidase (Figure 4A), 3.5 Å from the catalytic residue Glu-413, and contacts Asp-163, Val-446, Phe-448, Tyr-472, and Arg-562 within the active site region of the enzyme (Figure 5). Notably, in chain A it directly contacts Leu-361 of the "bacterial loop," a region that is unique to the microbial forms of the β-glucuronidase relative to the mammalian β-glucuronidases (Jain et al., 1996; Wallace et al., 2010). Inhibitor 8 binds in a manner similar to Inhibitors 2 and 3 elucidated previously in complexes with *E. coli* β-glucuronidase (Wallace et al., 2010), occupying a similar location in the enzyme and contacting 5 of the same residues (Figure 5). Indeed, the root-mean-square deviation between the Cα positions of the Inhibitor 2- and Inhibitor 8-bound structures of *E. coli* β-glucuronidase is 0.54 Å. However, while most residues contacted by Inhibitor 8 are in the same position in the Inhibitor 2 complex structure, the side chain of Leu-361 shifts by 3.6 Å. This observation suggests that the "bacterial loop" is capable of conforming to the presence of different bound inhibitors. Electron density in the simulated annealing omit and $2F_o$-F_c maps is less complete for Leu-361 in chain B compared to chain A.

Molecular Pharmacology Fast Forward. Published on May 20, 2013 as DOI: 10.1124/mol.113.085852
This article has not been copyedited and formatted. The final version may differ from this version.

The full "bacterial loop" of *E. coli* β-glucuronidase, residues 360-376, was visualized in the Inhibitor 2 and 3 co-crystal structures (Wallace et al., 2010); in complex with Inhibitor 8, though, only residues 372-376 are ordered with average B- factors less than 80 $Å^2$ (Figure 6A). In the absence of a bound ligand, the "bacterial loop" is not observed, as it gave no interpretable electron density in the structure of apo *E. coli* β-glucuronidase reported previously (Wallace et al., 2010). Thus, we conclude that *E. coli* β-glucuronidase can be inhibited effectively by compounds, like Inhibitor 8, capable of contacting only a portion of the loop unique to the microbial β-glucuronidases. In support of this conclusion, we found that a form of *E. coli* β-glucuronidase in which the "bacterial loop" was deleted, Δ360-376, was not inhibited by up to 100 μM of Inhibitors 5-8 (Figure 6B). The Δ360-376 *E. coli* β-glucuronidase exhibited comparable K_m (260 μM for Δ360-376, 360 μM for wild-type) values, but the V_{max} (2.44 nmol/sec for Δ360-376, 398 nmol/sec for wild-type) and k_{cat} (0.244 sec^{-1} for Δ360-376, 39.8 sec^{-1} for wild-type) values were reduced by approximately 2 orders of magnitude. Thus, the "bacterial loop" is essential for full activity of *E. coli* β-glucuronidase, as well as its selective inhibition.

Alleviation of CPT-11 Toxicity in Mice

Lastly, we tested the ability of the most potent compound examined in this study, Inhibitor 5 (K_i=180 nM, EC_{50}=300 nM), to alleviate CPT-11-induced intestinal toxicity in mice. We divided BALB/cJ female mice into four groups of nine animals each. Group 1 received an equivalent volume of only the vehicle (0.25% (w/v) carboxymethylcellulose sodium salt solution) intraperitoneally (i.p.) and by oral gavage twice per day. Group 2 received an oral gavage of Inhibitor 5 (10 μg/day) twice per day starting on day -1, as well as an i.p. injection of the vehicle solution once per day. Group 3 was injected with CPT-11 (50 mg/kg) i.p. once per day and received an oral gavage of the vehicle solution twice per day. Group 4 received both an injection of CPT-11 (50 mg/kg) once per day and an oral gavage of Inhibitor 5 (10 μg/day) twice per day.

Molecular Pharmacology Fast Forward. Published on May 20, 2013 as DOI: 10.1124/mol.113.085852
This article has not been copyedited and formatted. The final version may differ from this version.

The mice were observed and weighed daily, and were examined for incidence of diarrhea (Figure 7). Groups 1 and 2 showed no evidence of toxicity throughout the experiment. In group 3, GI symptoms were observed as early as day 2 and incidences of bloody diarrhea were observed in a third of the mice at day 8, and in all animals by day 10. In comparison, in group 4, where the mice were pretreated with Inhibitor 5, no mice showed evidence of bloody diarrhea by day 8 and less than 30% of mice showed symptoms by day 10 (Figure 7A).

The body weight of each mouse was also recorded each day during the course of the experiment (Figure 7B). Although Inhibitor 5 alleviated most of the toxicity associated with the CPT-11 treatment, it had no effect on the average body weight of the mice. Moreover, group 2, which only received treatment with Inhibitor 5, showed comparable body weights to the vehicle-only group, but had significantly higher body weights, starting at day 6, than group 4, which received treatment with Inhibitor 5 in addition to CPT-11. These data indicate that the presence of Inhibitor 5 significantly reduces the incidence of acute GI toxicity caused by CPT-11, and they suggest that Inhibitor 5 does not impact the systemic effects of this anticancer drug, as measured by weight loss.

Discussion

Research endeavors like the Human Microbiome Project continue to expand our appreciation of the roles the symbiotic microbiota play in mammalian physiology (Consortium, 2012). It also appears that widespread use of antibiotics may have subtle but serious side effects on human health (Maurice et al., 2013). Additionally, for patients with colorectal cancer, the use of antibiotics to treat CPT-11-induced toxicity may lead to the increased prevalence of subdominant bacterial species with higher overall β-glucuronidase activity in the GI tract, and thus, increased toxicity (Brandi et al., 2006). Studies have also shown that the long-term use of neomycin in mice leads to increased serum bilirubin that may interfere with proper hepatic CPT-11 metabolism (Vítek et al., 2005). These observations lead to the conclusion that the selective,

Molecular Pharmacology Fast Forward. Published on May 20, 2013 as DOI: 10.1124/mol.113.085852
This article has not been copyedited and formatted. The final version may differ from this version.

non-lethal inhibition of components of the GI microbiome will be an important method of enhancing drug efficacy and tolerance. In this report, we interrogate the roles bacterial β-glucuronidases play in mammalian GI drug toxicity by pharmacologically targeting this enzyme with potent and selective inhibitors.

Each of the compounds described, Inhibitors 5-8, exhibited strong *in vitro* inhibition of *E. coli* β-glucuronidase (Table 1) but did not affect the viability of either cultured bacterial or mammalian cells (Figure 3). Only Inhibitor 7 failed to disrupt β-glucuronidase activity in living *E. coli* cells. Furthermore, because compounds were ineffective against mammalian β-glucuronidase (Figure 2) and a range of enzymes from the glycosidase family, each inhibitor displayed selectivity toward *E. coli* β-glucuronidase. The selectivity of our inhibitors is particularly critical for their use in conjunction with CPT-11 because human β-glucuronidase expressed by tumor cells appears to play an important role in the anti-tumor efficacy of CPT-11 through the reactivation of SN-38G to SN-38 in the tumor microenvironment (Tobin et al., 2006; Huang et al., 2011). Of the four compounds described here, only Inhibitor 5 (K_i and IC_{50} values of 180 and 540 nM, respectively) displayed potency comparable to our previously-characterized inhibitors, which have a scaffold not shared by the four inhibitors outlined in this study (Wallace et al., 2010). As such, these data advance our understanding of the chemical moieties capable of selective bacterial β-glucuronidase inhibition.

We successfully determined the x-ray crystal structure of one of our inhibitors (Inhibitor 8) in complex with *E. coli* β-glucuronidase (Figure 4). This adds to our knowledge of *E. coli* β-glucuronidase inhibition that started with the structures of the complexes of Inhibitors 2 and 3 reported previously (Wallace et al., 2010). Similar to those structures, Inhibitor 8 binds at the entrance to the active site cleft and forms related contacts, including one with the catalytic glutamic acid residue, Glu-413. Importantly, Inhibitor 8 also makes a hydrophobic contact with Leu-361, which is part of the “bacterial loop” unique to the microbial enzymes. Overlaying the structures of the complexes with Inhibitor 2 and Inhibitor 8, it is apparent that Leu-361 has

Molecular Pharmacology Fast Forward. Published on May 20, 2013 as DOI: 10.1124/mol.113.085852
This article has not been copyedited and formatted. The final version may differ from this version.

shifted to facilitate binding, suggesting that bacterial loop flexibility is involved in inhibition (Figure 6). The observation that the bacterial loop in the Inhibitor 8 complex structure is disordered for the eight residues C-terminal to Leu-361 supports that conclusion. Mutagenesis studies in which the bacterial loop has been deleted confirm its importance in microbial β-glucuronidase inhibition (Figure 6).

Lastly, only the previously reported Inhibitor 1 had been examined to date in drug-induced GI toxicity studies in mice (Wallace et al., 2010; LoGuidice et al., 2012). In this report, we tested the *in vivo* efficacy our most effective compound outlined here, Inhibitor 5, in a mouse model of CPT-11 toxicity (Figure 7). Groups of BALB/cJ mice were dosed with Inhibitor 5, CPT-11, or a combination of both. The group that received CPT-11 alone developed bloody diarrhea by day 8, and 100% of the mice showed signs of this toxicity by day 10. The group that was treated with Inhibitor 5 orally, along with CPT-11 by i.p., had significantly fewer incidents of bloody diarrhea compared to the CPT-11 group, highlighting the protective effects of Inhibitor 5. It is also interesting to note that the mice that received CPT-11 lost body weight at the same rate regardless of treatment with Inhibitor 5. This suggests that Inhibitor 5 protected against CPT-11-induced GI toxicity but that the systemic pharmacodynamics of CPT-11 in the mouse are not impacted. A more comprehensive examination of tumor xenografts and pharmacokinetics will be required to substantiate this conclusion.

We have described the inhibitory profile of a range of chemically-distinct compounds and assessed their potential as orally delivered pharmacological agents. They are *in vitro* inhibitors to *E. coli* β-glucuronidase and, with the exception of Inhibitor 7, are also effective in *E. coli* cells. Moreover, our inhibitors appear to be selective for bacterial β-glucuronidase and non-lethal to bacterial and mammalian cells. The structural data presented here, along with the data from our previously-characterized inhibitors, will allow us to better understand their mechanism of selective microbial β-glucuronidase inhibition. As such, they may facilitate the development of

Molecular Pharmacology Fast Forward. Published on May 20, 2013 as DOI: 10.1124/mol.113.085852
This article has not been copyedited and formatted. The final version may differ from this version.

therapeutics capable of alleviating drug-induced GI toxicity generated by symbiotic microbial β-glucuronidases.

Molecular Pharmacology Fast Forward. Published on May 20, 2013 as DOI: 10.1124/mol.113.085852
This article has not been copyedited and formatted. The final version may differ from this version.

Authorship Contributions

Participated in research design: Roberts, Wallace, Kumar, Mani, Redinbo

Conducted experiments: Roberts, Wallace, Kumar

Data analysis: Roberts, Wallace, Kumar, Mani, Redinbo

Wrote and contributed to manuscript: Roberts, Kumar, Mani, Redinbo

Molecular Pharmacology Fast Forward. Published on May 20, 2013 as DOI: 10.1124/mol.113.085852
This article has not been copyedited and formatted. The final version may differ from this version.

References

Abigerges D, Armand JP, Chabot GG, Da Costa L, Fadel E, Cote C, Hérait P, Gandia D (1994) Irinotecan (CPT-11) high-dose escalation using intensive high-dose loperamide to control diarrhea. *J Natl Cancer Inst* **86**: 446–449

Adams PD, Grosse-Kunstleve RW, Hung LW, Ioerger TR, McCoy AJ, Moriarty NW, Read RJ, Sacchettini JC, Sauter NK, Terwilliger TC (2002) PHENIX: building new software for automated crystallographic structure determination. *Acta Crystallogr D Biol Crystallogr* **58**: 1948–1954

Ahmad S, Hughes MA, Lane KT, Redinbo MR, Yeh L-A, Scott JE (2011) A High Throughput Assay for Discovery of Bacterial β-Glucuronidase Inhibitors. *Curr Chem Genomics* **5**: 13–20

Araki E, Ishikawa M, Iigo M, Koide T, Itabashi M, Hoshi A (1993) Relationship between Development of Diarrhea and the Concentration of SN-38, an Active Metabolite of CPT-11, in the Intestine and the Blood Plasma of Athymic Mice Following Intraperitoneal Administration of CPT-11. *Cancer Science* **84**: 697–702

Brandi G, Dabard J, Raibaud P, Di Battista M, Bridonneau C, Pisi AM, Morselli Labate AM, Pantaleo MA, De Vivo A, Biasco G (2006) Intestinal microflora and digestive toxicity of irinotecan in mice. *Clin Cancer Res* **12**: 1299–1307

Brünger AT (1997) Free R value: cross-validation in crystallography. *Meth Enzymol* **277**: 366–396

Consortium THMP (2012) Structure, function and diversity of the healthy human microbiome. *Nature* **486**: 207–214

Cooper HS, Murthy SN, Shah RS, Sedergran DJ (1993) Clinicopathologic study of dextran sulfate sodium experimental murine colitis. *Lab Invest* **69**: 238–249

Cunningham D, Pyrhönen S, James RD, Punt CJ, Hickish TF, Heikkila R, Johannesen TB, Starkhammar H, Topham CA, Awad L, et al (1998) Randomised trial of irinotecan plus supportive care versus supportive care alone after fluorouracil failure for patients with metastatic colorectal cancer. *Lancet* **352**: 1413–1418

Ducreux M, Köhne C-H, Schwartz GK, Vanhoefer U (2003) Irinotecan in metastatic colorectal cancer: dose intensification and combination with new agents, including biological response modifiers. *Ann Oncol* **14 Suppl 2**: ii17–23

Emsley P, Cowtan K (2004) Coot: model-building tools for molecular graphics. *Acta Crystallogr D Biol Crystallogr* **60**: 2126–2132

Fuchs CS, Moore MR, Harker G, Villa L, Rinaldi D, Hecht JR (2003) Phase III Comparison of Two Irinotecan Dosing Regimens in Second-Line Therapy of Metastatic Colorectal Cancer. *Journal of Clinical Oncology* **21**: 807 –814

Graef V, Furuya E, Nishikaze O (1977) Hydrolysis of steroid glucuronides with beta-glucuronidase preparations from bovine liver, Helix pomatia, and E. coli. *Clin Chem* **23**: 532–535

Han J-Y, Shin ES, Lee Y-S, Ghang HY, Kim S-Y, Hwang J-A, Kim JY, Lee JS (2012) A genome-wide association study for irinotecan-related severe toxicities in patients with advanced non-small-cell lung cancer. *Pharmacogenomics J*. doi: 10.1038/tpj.2012.24

Hu Z-P, Yang X-X, Chan SY, Xu A-L, Duan W, Zhu Y-Z, Sheu F-S, Boelsterli UA, Chan E, Zhang Q, et al (2006) St. John's wort attenuates irinotecan-induced diarrhea via down-regulation of intestinal pro-inflammatory cytokines and inhibition of intestinal epithelial apoptosis. *Toxicology and Applied Pharmacology* **216**: 225–237

Huang P-T, Chen K-C, Prijovich ZM, Cheng T-L, Leu Y-L, Roffler SR (2011) Enhancement of CPT-11 antitumor activity by adenovirus-mediated expression of β–glucuronidase in tumors. *Cancer Gene Therapy* **18**: 381–389

Jain S, Drendel WB, Chen ZW, Mathews FS, Sly WS, Grubb JH (1996) Structure of human beta-glucuronidase reveals candidate lysosomal targeting and active-site motifs. *Nat Struct Biol* **3**: 375–381

Jo J-C, Lee J-L, Ryu M-H, Chang HM, Kim M, Lee HJ, Kim H-S, Shin J-G, Kim T-W, Kang Y-K (2012) Phase II and UGT1A1 genotype study of irinotecan dose escalation as salvage therapy for advanced gastric cancer. *British journal of cancer* **106**: 1591–1597

Kambe M, Kikuchi H, Gamo M, Yoshioka T, Ohashi Y, Kanamaru R (2012) Phase I study of irinotecan by 24-h intravenous infusion in combination with 5-fluorouracil in metastatic colorectal cancer. *Int J Clin Oncol* **17**: 150–154

Kawato Y, Aonuma M, Hirota Y, Kuga H, Sato K (1991) Intracellular roles of SN-38, a metabolite of the camptothecin derivative CPT-11, in the antitumor effect of CPT-11. *Cancer Res* **51**: 4187–4191

Kim A, Ueda Y, Naka T, Enomoto T (2012) Therapeutic strategies in epithelial ovarian cancer. *J Exp Clin Cancer Res* **31**: 14

Kurita A, Kado S, Matsumoto T, Asakawa N, Kaneda N, Kato I, Uchida K, Onoue M, Yokokura T (2011) Streptomycin alleviates irinotecan-induced delayed-onset diarrhea in rats by a mechanism other than inhibition of β-glucuronidase activity in intestinal lumen. *Cancer Chemother Pharmacol* **67**: 201–213

Lee KS, Park IH, Nam B-H, Ro J (2013) Phase II study of irinotecan plus capecitabine in anthracycline- and taxane- pretreated patients with metastatic breast cancer. *Invest New Drugs* **31**: 152–159

LoGuidice A, Wallace BD, Bendel L, Redinbo MR, Boelsterli UA (2012) Pharmacologic targeting of bacterial β-glucuronidase alleviates nonsteroidal anti-inflammatory drug-induced enteropathy in mice. *J Pharmacol Exp Ther* **341**: 447–454

Ma MK, McLeod HL (2003) Lessons learned from the irinotecan metabolic pathway. *Curr Med Chem* **10**: 41–49

Mathijssen RH, van Alphen RJ, Verweij J, Loos WJ, Nooter K, Stoter G, Sparreboom A (2001) Clinical pharmacokinetics and metabolism of irinotecan (CPT-11). *Clin Cancer Res* **7**: 2182–2194

Matsumura M, Takeshima N, Ota T, Omatsu K, Sakamoto K, Kawamata Y, Umayahara K, Tanaka H, Akiyama F, Takizawa K (2010) Neoadjuvant chemotherapy followed by radical hysterectomy plus postoperative chemotherapy but no radiotherapy for Stage IB2-IIB cervical cancer--irinotecan and platinum chemotherapy. *Gynecol Oncol* **119**: 212–216

Maurice CF, Haiser HJ, Turnbaugh PJ (2013) Xenobiotics shape the physiology and gene expression of the active human gut microbiome. *Cell* **152**: 39–50

McCoy AJ, Grosse-Kunstleve RW, Adams PD, Winn MD, Storoni LC, Read RJ (2007) Phaser crystallographic software. *J Appl Crystallogr* **40**: 658–674

Nagar S, Blanchard RL (2006) Pharmacogenetics of uridine diphosphoglucuronosyltransferase (UGT) 1A family members and its role in patient response to irinotecan. *Drug Metab Rev* **38**: 393–409

Ray J, Scarpino V, Laing C, Haskins ME (1999) Biochemical basis of the beta-glucuronidase gene defect causing canine mucopolysaccharidosis VII. *J Hered* **90**: 119–123

Reagan-Shaw S, Nihal M, Ahmad N (2008) Dose translation from animal to human studies revisited. *FASEB J* **22**: 659–661

Rothenberg ML, Eckardt JR, Kuhn JG, Burris HA 3rd, Nelson J, Hilsenbeck SG, Rodriguez GI, Thurman AM, Smith LS, Eckhardt SG, et al (1996) Phase II trial of irinotecan in patients with progressive or rapidly recurrent colorectal cancer. *J Clin Oncol* **14**: 1128–1135

Rougier P, Bugat R, Douillard JY, Culine S, Suc E, Brunet P, Becouarn Y, Ychou M, Marty M, Extra JM, et al (1997) Phase II study of irinotecan in the treatment of advanced colorectal cancer in chemotherapy-naive patients and patients pretreated with fluorouracil-based chemotherapy. *J Clin Oncol* **15**: 251–260

Rougier P, Van Cutsem E, Bajetta E, Niederle N, Possinger K, Labianca R, Navarro M, Morant R, Bleiberg H, Wils J, et al (1998) Randomised trial of irinotecan versus fluorouracil by continuous infusion after fluorouracil failure in patients with metastatic colorectal cancer. *Lancet* **352**: 1407–1412

Saliba F, Hagipantelli R, Misset JL, Bastian G, Vassal G, Bonnay M, Herait P, Cote C, Mahjoubi M, Mignard D, et al (1998) Pathophysiology and therapy of irinotecan-induced delayed-onset diarrhea in patients with advanced colorectal cancer: a prospective assessment. *J Clin Oncol* **16**: 2745–2751

Saltz LB, Cox JV, Blanke C, Rosen LS, Fehrenbacher L, Moore MJ, Maroun JA, Ackland SP, Locker PK, Pirotta N, et al (2000) Irinotecan plus fluorouracil and leucovorin for metastatic colorectal cancer. Irinotecan Study Group. *N Engl J Med* **343**: 905–914

Schüttelkopf AW, van Aalten DMF (2004) PRODRG: a tool for high-throughput crystallography of protein-ligand complexes. *Acta Crystallogr D Biol Crystallogr* **60**: 1355–1363

Smith NF, Figg WD, Sparreboom A (2006) Pharmacogenetics of irinotecan metabolism and transport: an update. *Toxicol In Vitro* **20**: 163–175

Sousa T, Paterson R, Moore V, Carlsson A, Abrahamsson B, Basit AW (2008) The gastrointestinal microbiota as a site for the biotransformation of drugs. *Int J Pharm* **363**: 1–25

Spigel DR, Greco FA, Rubin MS, Shipley D, Thompson DS, Lubiner ET, Eakle JF, Quinn R, Burris HA, Hainsworth JD (2012) Phase II study of maintenance sunitinib following irinotecan and carboplatin as first-line treatment for patients with extensive-stage small-cell lung cancer. *Lung Cancer* **77**: 359–364

Stein A, Voigt W, Jordan K (2010) Chemotherapy-induced diarrhea: pathophysiology, frequency and guideline-based management. *Ther Adv Med Oncol* **2**: 51–63

Takasuna K, Hagiwara T, Hirohashi M, Kato M, Nomura M, Nagai E, Yokoi T, Kamataki T (1996) Involvement of beta-glucuronidase in intestinal microflora in the intestinal toxicity of the antitumor camptothecin derivative irinotecan hydrochloride (CPT-11) in rats. *Cancer Res* **56**: 3752–3757

Takasuna K, Hagiwara T, Hirohashi M, Kato M, Nomura M, Nagai E, Yokoi T, Kamataki T (1998) Inhibition of intestinal microflora beta-glucuronidase modifies the distribution of the active metabolite of the antitumor agent, irinotecan hydrochloride (CPT-11) in rats. *Cancer Chemother Pharmacol* **42**: 280–286

Tobin P, Clarke S, Seale JP, Lee S, Solomon M, Aulds S, Crawford M, Gallagher J, Eyers T, Rivory L (2006) The in vitro metabolism of irinotecan (CPT-11) by carboxylesterase and beta-glucuronidase in human colorectal tumours. *Br J Clin Pharmacol* **62**: 122–129

Tobin PJ, Dodds HM, Clarke S, Schnitzler M, Rivory LP (2003) The relative contributions of carboxylesterase and beta-glucuronidase in the formation of SN-38 in human colorectal tumours. *Oncol Rep* **10**: 1977–1979

Vítek L, Zelenka J, Zadinová M, Malina J (2005) The impact of intestinal microflora on serum bilirubin levels. *J Hepatol* **42**: 238–243

Wallace BD, Wang H, Lane KT, Scott JE, Orans J, Koo JS, Venkatesh M, Jobin C, Yeh L-A, Mani S, et al (2010) Alleviating cancer drug toxicity by inhibiting a bacterial enzyme. *Science* **330**: 831–835

Z. Otwinowski, W. Minor, Charles W. Carter, Jr. (1997) *Methods Enzymol*. Academic Press

Zaniboni A, Aitini E, Barni S, Ferrari D, Cascinu S, Catalano V, Valmadre G, Ferrara D, Veltri E, Codignola C, et al (2012) FOLFIRI as second-line chemotherapy for advanced pancreatic cancer: a GISCAD multicenter phase II study. *Cancer Chemother Pharmacol* **69**: 1641–1645

Zhao J, Huang L, Belmar N, Buelow R, Fong T (2004) Oral RDP58 allows CPT-11 dose intensification for enhanced tumor response by decreasing gastrointestinal toxicity. *Clin Cancer Res* **10**: 2851–2859

Footnotes:

This work was funded by the National Institutes of Health [Grants CA98468, CA161879, CA127231]; and the UNC Translational Medicine Training Program.

Molecular Pharmacology Fast Forward. Published on May 20, 2013 as DOI: 10.1124/mol.113.085852
This article has not been copyedited and formatted. The final version may differ from this version.

Figure Legends

Figure 1. Chemical structures of the Inhibitors 1-8.

Figure 2. Impact of increasing concentrations of Inhibitors 5-8 on the activity of bovine β-glucuronidase.

Figure 3. Impact of Inhibitors 5-8 at 100 μM on the survival of *E. coli* (**A**) and HCT116 cells (**B**). Ampicillin and 10% Triton-X100 are used as positive controls for microbial and human cell lethality, respectively. Additionally, 2% DMSO, in which the inhibitors are solubilized, is also shown.

Figure 4. A. Crystal structure of the *E. coli* β-glucuronidase dimer in complex with Inhibitor 8 (PDB ID 4JHZ). **B.** Composite annealing omit (σA-weighted) 2.8 Å resolution electron density contoured at 1.0 σ for Inhibitor 8 in the active site of each monomer of *E. coli* β-glucuronidase.

Figure 5. Contacts formed by Inhibitor 8 (pink) at the active site of *E. coli* β-glucuronidase. Inhibitor 2 (yellow) from a previously resolved structure is also shown, as are the side chains for the Inhibitor 8 and Inhibitor 2 complexes (blue and purple, respectively).

Figure 6. **A.** Bound Inhibitor 8 (pink) adjacent to the largely disordered "bacterial loop" of *E. coli* β-glucuronidase (blue). The completely ordered "bacterial loop" of *E. coli* β-glucuronidase (purple) in complex with Inhibitor 2 (yellow) is overlaid for comparison. The image is in the same orientation as Figure 5 **B.** Inhibitors 5-8 at 100 μM inhibit wild-type (WT) *E. coli* β-glucuronidase, but not a mutant *E. coli* β-glucuronidase in which the "bacterial loop" (residues 360-376) has been deleted.

Molecular Pharmacology Fast Forward. Published on May 20, 2013 as DOI: 10.1124/mol.113.085852
This article has not been copyedited and formatted. The final version may differ from this version.

Figure 7. A. Groups of nine BALB/cJ mice were dose with either vehicle, Inhibitor 5, CPT-11, or pre-treated with Inhibitor 5 followed by CPT-11, and then examined for incidences of CPT-11-induced toxicity (i.e., bloody diarrhea). **B**. The mice were weighed daily. Administration of CPT-11 incited the loss of body weight during treatment. Oral administration of Inhibitor 5 had no protective effects on body weight during CPT-11 treatment. The Inhibitor 5 only and CPT-11 + Inhibitor 5 groups were analyzed for statistical significance. **, $p < 0.01$ and ***, $p < 0.001$

Molecular Pharmacology Fast Forward. Published on May 20, 2013 as DOI: 10.1124/mol.113.085852
This article has not been copyedited and formatted. The final version may differ from this version.

Table 1. *In vitro* and cell-based assays for β-glucuronidase activity and inhibitor efficacy. Errors represent standard error, where N = 3. NI, no inhibition

	E. coli β-glucuronidase *in vitro*		*E. coli* cell-based
	K_i (nM)	IC_{50} (nM)	EC_{50} (nM)
Inhibitor 5	217 ± 42.6	542 ± 93.7	306 ± 8.35
Inhibitor 6	668 ± 28.8	8890 ± 2930	747 ± 167
Inhibitor 7	1920 ± 21.0	14900 ± 2530	NI
Inhibitor 8	957 ± 22.8	6430 ± 1380	1200 ± 256

Molecular Pharmacology Fast Forward. Published on May 20, 2013 as DOI: 10.1124/mol.113.085852
This article has not been copyedited and formatted. The final version may differ from this version.

Table 2

X-ray source	APS ANL, SER-CAT, 22-ID
Space group	C2
Unit cell: a, b, c (Å); α, β, γ (°)	168.3, 77.4, 126.3; 90, 124.8, 90
Resolution range (Å) (highest shell)	41.80 - 2.83 (2.933 - 2.83)
Wavelength (Å)	1.00
Unique reflections	31648 (3115)
Multiplicity	4.1 (3.7)
Completeness (%)	98.82 (96.98)
I/σ	10.09 (2.22)
Wilson B-factor	59.72
R_{work}	0.1964 (0.2653)
R_{free}	0.2438 (0.3286)
Molecules per asymmetric unit (AU)	2
No. of waters per AU	124
No. of protein residues per AU	1192
Average *B*-factor	70.80
RMS (bond lengths)	0.006
RMS (bond angles)	1.02
Ramachandran favored (%)	93
Ramachandran outliers (%)	0.42

Figure 1

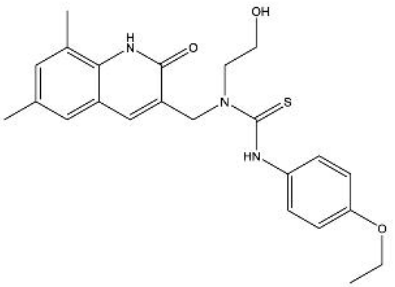

Inhibitor 1

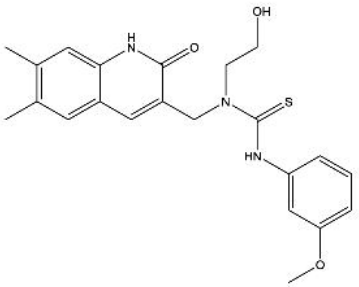

Inhibitor 2

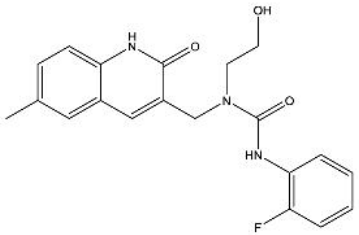

Inhibitor 3

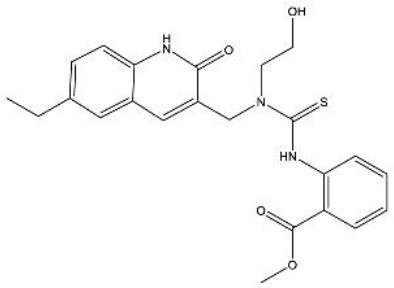

Inhibitor 4

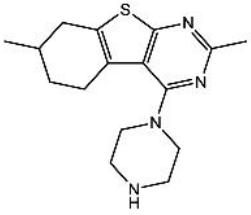

Inhibitor 5

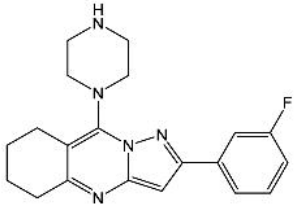

Inhibitor 6

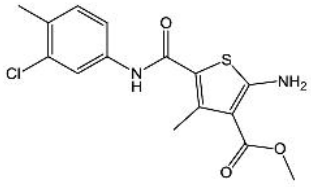

Inhibitor 7

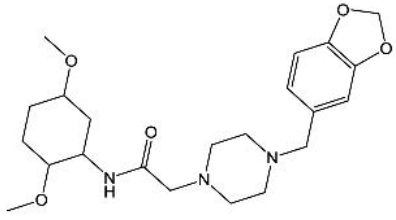

Inhibitor 8

Figure 2

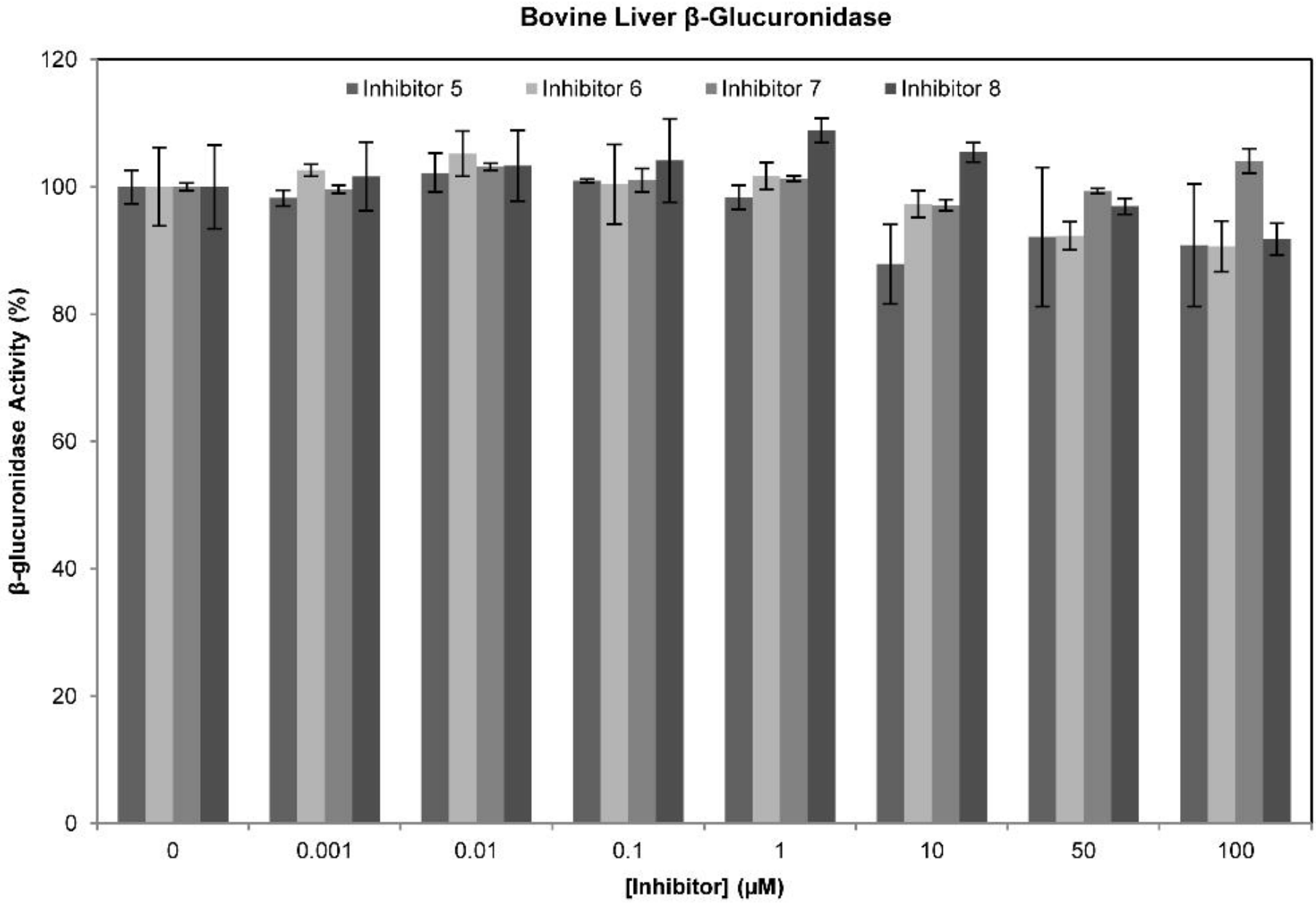
Bovine Liver β-Glucuronidase
Inhibitor 5
Inhibitor 6
Inhibitor 7
Inhibitor 8
β-glucuronidase Activity (%)
120
100
80
60
40
20
0
0
0.001
0.01
0.1
1
10
50
100
[Inhibitor] (μM)

Figure 3

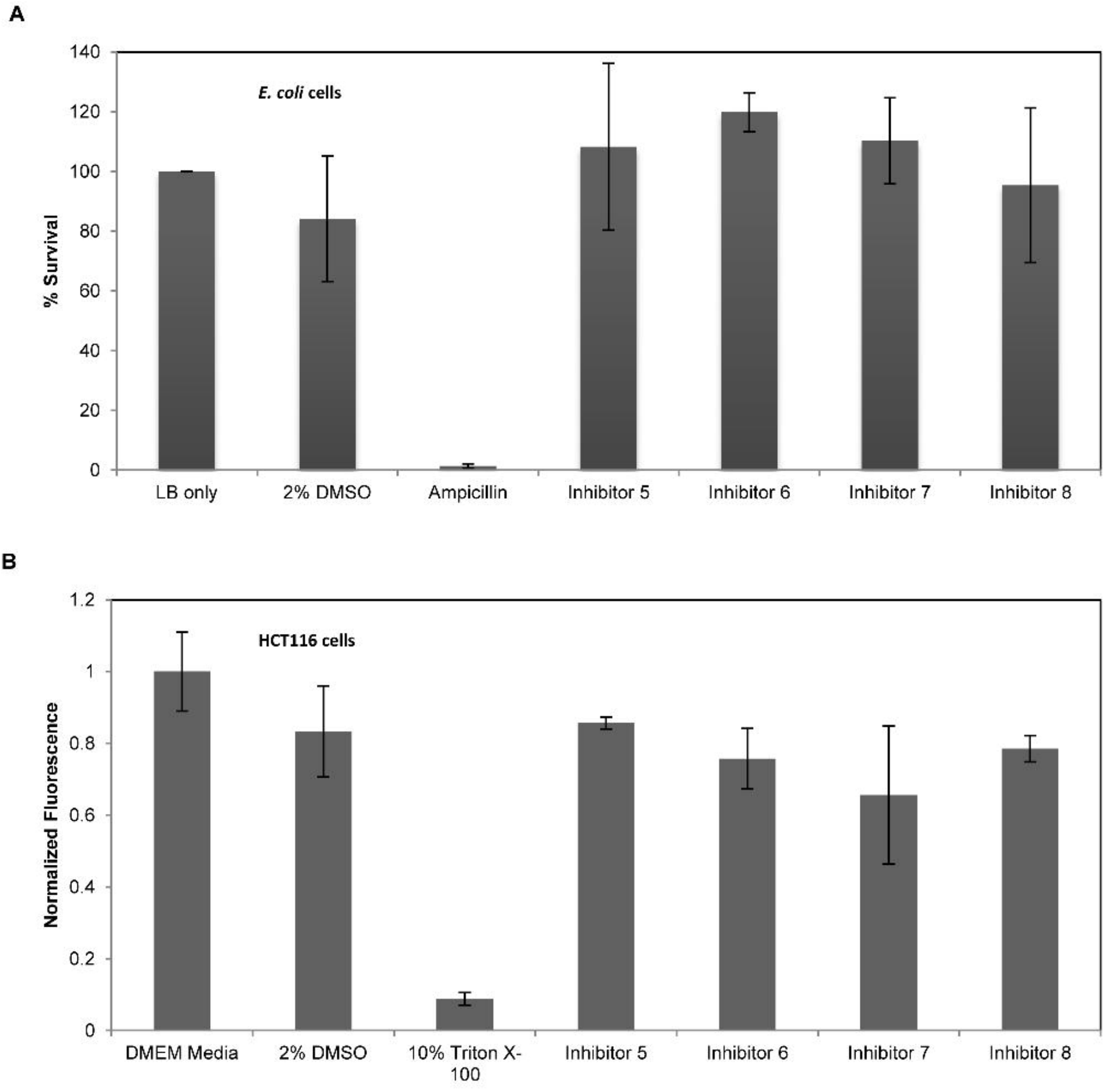
A
E. coli cells
% Survival
140
120
100
80
60
40
20
0
LB only
2% DMSO
Ampicillin
Inhibitor 5
Inhibitor 6
Inhibitor 7
Inhibitor 8
B
HCT116 cells
Normalized Fluorescence
1.2
1
0.8
0.6
0.4
0.2
0
DMEM Media
2% DMSO
10% Triton X-100
Inhibitor 5
Inhibitor 6
Inhibitor 7
Inhibitor 8

Figure 4

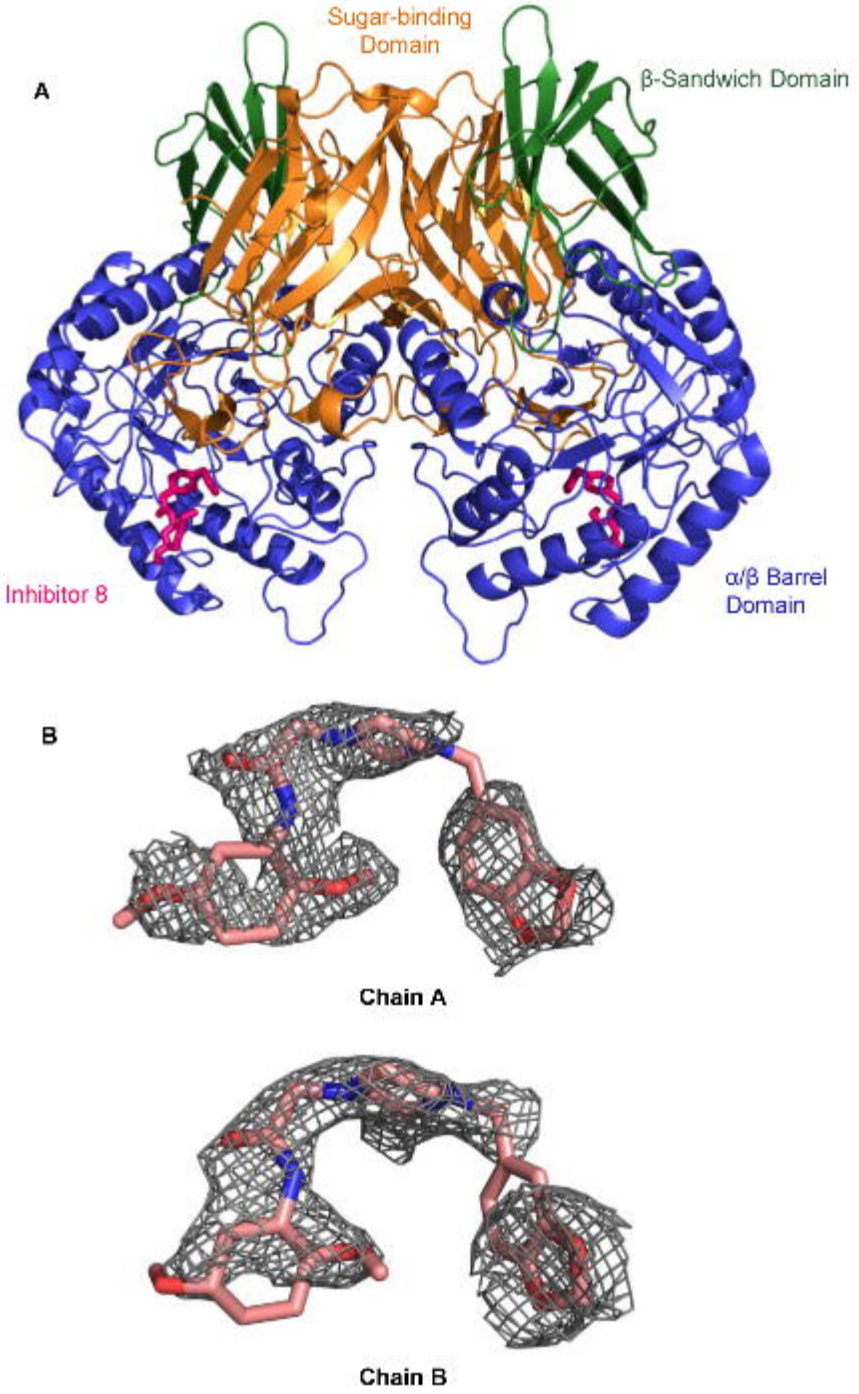
A
Sugar-binding Domain
β-Sandwich Domain
Inhibitor 8
α/β Barrel Domain
B
Chain A
Chain B

Figure 5

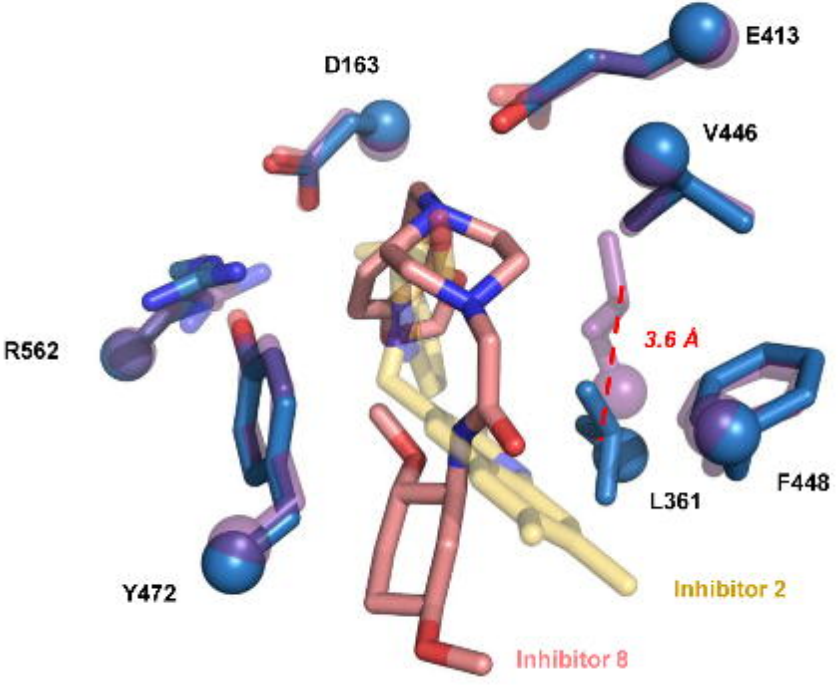
E413
D163
V446
R562
3.6 Å
F448
L361
Y472
Inhibitor 2
Inhibitor 8

Figure 6

A

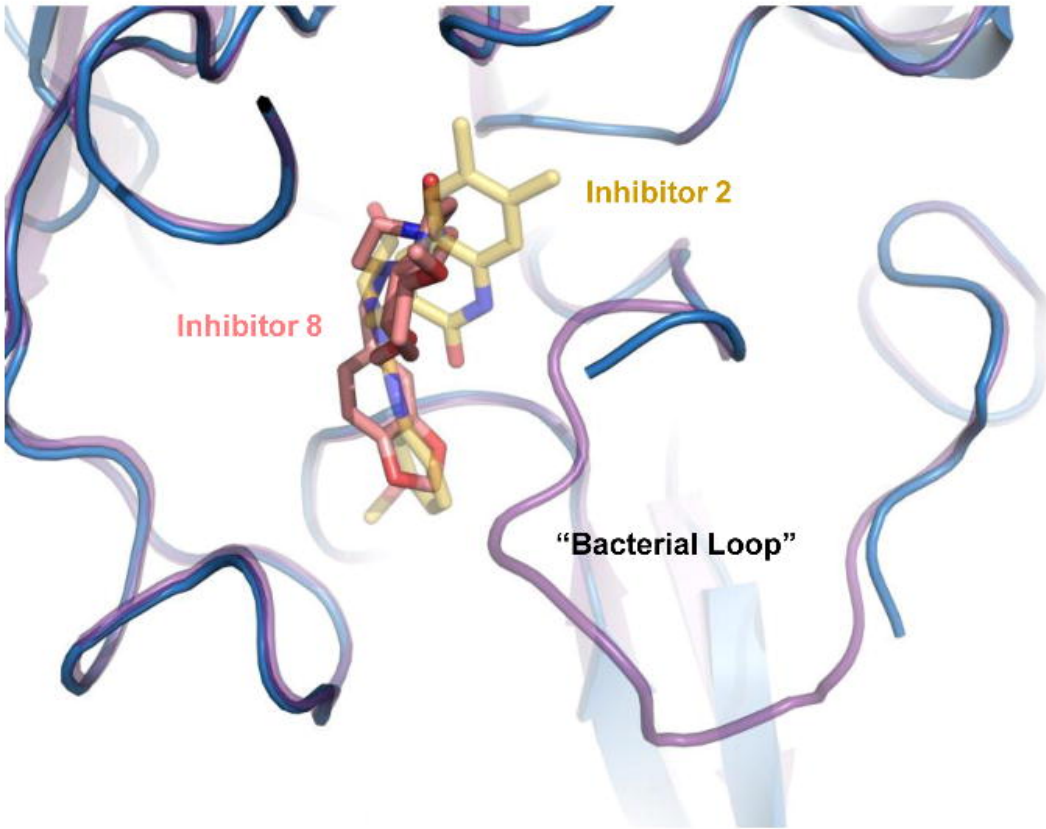
Inhibitor 2
Inhibitor 8
"Bacterial Loop"

B

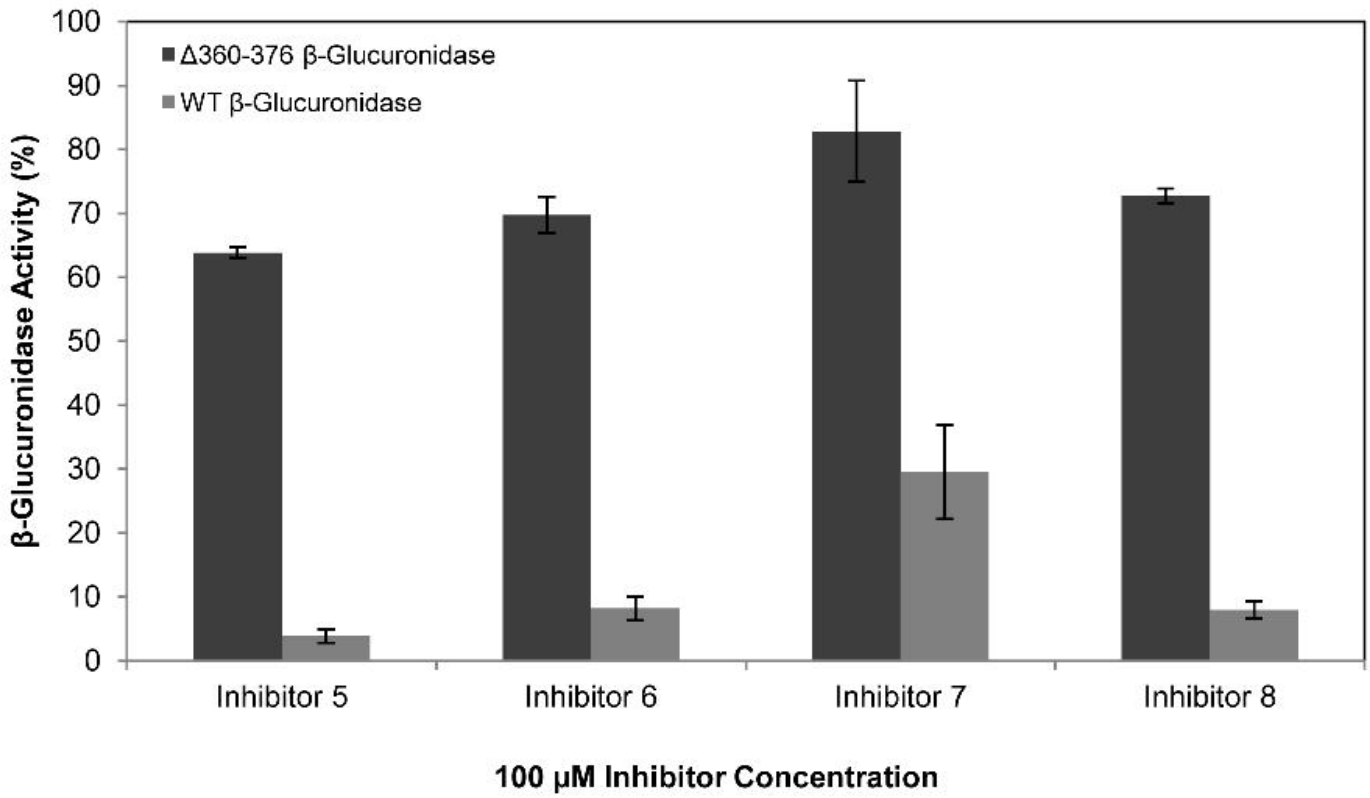
Δ360-376 β-Glucuronidase
WT β-Glucuronidase
β-Glucuronidase Activity (%)
100
90
80
70
60
50
40
30
20
10
0
Inhibitor 5
Inhibitor 6
Inhibitor 7
Inhibitor 8
100 μM Inhibitor Concentration

Figure 7

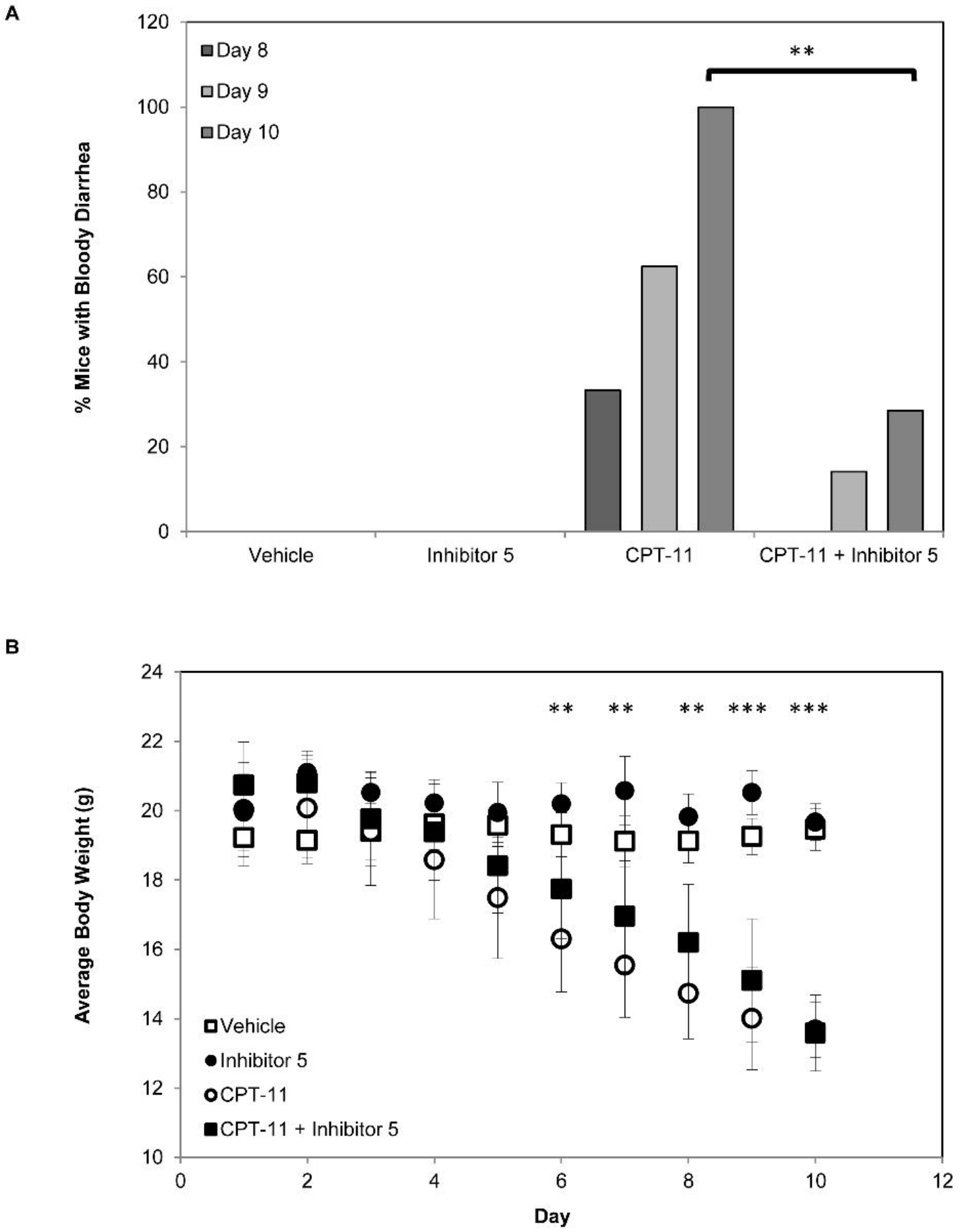
A
120
100
80
60
40
20
0
% Mice with Bloody Diarrhea
Day 8
Day 9
Day 10
**
Vehicle
Inhibitor 5
CPT-11
CPT-11 + Inhibitor 5
B
24
22
20
18
16
14
12
10
Average Body Weight (g)
** ** ** *** ***
Vehicle
Inhibitor 5
CPT-11
CPT-11 + Inhibitor 5
0
2
4
6
8
10
12
Day